The EMBO Journal vol.13 no.16 pp.3661-3668, 1994

The crystal structure of elongation factor G complexed with GDP, at 2.7 Å resolution

J.Czworkowski[1], J.Wang[2], T.A.Steitz[1,2,3] and P.B.Moore[1,2,4]

Departments of [1]Chemistry, [2]Molecular Biophysics and Biochemistry and [3]Howard Hughes Medical Institute, Yale University, New Haven, CT 06520, USA

[4]Corresponding author

Communicated by J.A.Steitz

Elongation factor G (EF-G) catalyzes the translocation step of protein synthesis in bacteria, and like the other bacterial elongation factor, EF-Tu—whose structure is already known—it is a member of the GTPase superfamily. We have determined the crystal structure of EF-G–GDP from *Thermus thermophilus*. It is an elongated molecule whose large, N-terminal domain resembles the G domain of EF-Tu, except for a 90 residue insert, which covers a surface that is involved in nucleotide exchange in EF-Tu and other G proteins. The tertiary structures of the second domains of EF-G and EF-Tu are nearly identical, but the relative placement of the first two domains in EF-G–GDP resembles that seen in EF-Tu–GTP, not EF-Tu–GDP. The remaining three domains of EF-G look like RNA binding domains, and have no counterparts in EF-Tu.

Key words: elongation factor/EF-G/G protein

Introduction

Two protein factors participate in the elongation phase of bacterial protein synthesis, elongation factor Tu (EF-Tu) and elongation factor G (EF-G). Their eukaryotic homologs are EF-1 and EF-2, respectively (Nathans and Lipmann, 1961; Allende *et al.*, 1964; Arlinghaus *et al.*, 1964; Nizushima and Lipmann, 1966). EF-Tu delivers aminoacyl tRNAs to the A site of elongating ribosomes, and EF-G catalyzes translocation (see Spirin, 1985). During translocation, peptidyl tRNA moves from the A site to the P site of the ribosome, ribosomes advance along mRNAs by one codon (Gupta *et al.*, 1971; Thach and Thach, 1971), discharged tRNAs move from the P site to the E site (Rheinberger *et al.*, 1990), and EF-G bound GTP is cleaved to GDP and phosphate (Kaziro, 1978). Since the ribosomai sites for EF-Tu and EF-G overlap (Richman and Bodley, 1972), EF-G–GDP must dissociate from the ribosome before the next amino acid can be incorporated.

Neither EF-G nor EF-Tu imparts to the ribosome a capability it would otherwise lack. Messenger RNA directed binding of aminoacyl tRNAs to the ribosomal A site can occur in the absence of EF-Tu, and translocation will take place without the participation of EF-G (Gavrilova *et al.*, 1976). EF-G's role in protein synthesis is thus to accelerate protein synthesis by reducing the activation barrier that separates the pre- and post-translocational states of the ribosome (Schilling-Bartetzko *et al.*, 1992).

EF-Tu and EF-G are both members of the GTPase superfamily that includes $p21^{ras}$ (Bourne *et al.*, 1991). The ribosome activates the GTPase activity of both; it is their 'activating protein' (GAP). The replacement of GDP with GTP in the nucleotide binding site of EF-Tu is promoted by elongation factor Ts (EF-Ts), and similar guanine nucleotide release proteins (GNRPs) exist for other G proteins, but not for EF-G. EF-G binds GDP and GTP with about the same affinity as EF-Tu–EF-Ts, which is about 500 times less tightly than EF-Tu alone (Arai *et al.*, 1978).

As a step towards the elucidation of the mechanism of translocation, we have undertaken an investigation of the crystal structure of EF-G–GDP from *Thermus thermophilus*, the results of which are reported below. The conformation of nucleotide-free EF-G from the same organism has also just been determined; the outcome of that investigation is reported in a companion paper (Ævarsson *et al.*, 1994).

Results

Determination of the structure of EF-G–GDP

EF-G–GDP from *T.thermophilus* crystallizes in the space group $P2_12_12_1$, with unit cell dimensions of a=75.9 Å, b=104.0 Å, c=115.7 Å, and one molecule per asymmetric unit (see Materials and methods). These EF-G–GDP crystals shatter when handled and they had to be stabilized by cross-linking with glutaraldehyde (Quiocho and Richards, 1964) before anything could be done with them. This reduced the resolution to which they diffract; the best cross-linked crystals obtained so far diffract to only 2.7 Å, but unfixed crystal fragments diffract to 2.2 Å. Cross-linking may also have contributed to a crystal-to-crystal variability that made it hard to merge data sets.

Phases were obtained using isomorphous replacement and anomalous scattering; crystallographic statistics are summarized in Table I. The mercurials used to make heavy atom derivatives (see Materials and methods) react with EF-G at several sites, all of them close to C72. Electron density maps phased by single isomorphous replacement and anomalous scattering were not much worse than maps phased with multiple derivatives and anomalous scattering. The boundary of the molecule and many of its secondary structure elements could be seen in the initial, experimentally phased, electron density maps. Once phases had been improved by solvent-flattening and histogram matching (Wang, 1985; Zhang, 1993), it became possible to build the sequence (Yakhnin *et al.*, 1989) into the map.

At this point, refinement against a native data set to 2.7 Å has led to an electron density map in which it has

been possible to place 593 of the molecule's 691 side chains. The course of its backbone has been traced for another 64 residues, and 34 residues are assigned to disordered regions. The current structure, which includes no water molecules and has separate, overall temperature factors for each domain, has an *R* factor of 27%. Bond lengths and bond angles deviate from nominal by 0.013 Å r.m.s.d. and 2.0° r.m.s.d., respectively. Figure 1 shows the refined structure in the neighborhood of the GDP, superimposed on the electron density map that resulted from MIR phasing and solvent flattening.

It is interesting to note that a platinum derivative of EF-G–GDP we prepared, which was so non-isomorphous with existing native crystals as to have almost no phasing power at all, proved helpful in fitting the sequence into the electron density map. A difference Fourier map calculated using that derivative had clear, positive peaks at eight sites: the site where mercury binds (which includes C72, H359 and H362) and seven methionine sites (M98, M183, M228, M317, M358, M588 and M671).

Table I. Crystallographic statistics

Crystal	Resolution (Å)	R_{sym} (%)	R_F (%)	No. of sites	$\langle f_H \rangle / \langle E \rangle$
Native #2	2.85	6.0			
Native #3	2.7	5.1			
Baker's	3.3	7.9	16.8	4	1.93
DMNP	2.9	7.7	12.0	1	1.26

Mean figure of merit (F. of M.) versus resolution:

Resolution (Å)	>21.72	11.48	7.80	5.91	4.76	3.98	3.42	3.00	overall
F. of M.	0.69	0.92	0.94	0.93	0.89	0.80	0.71	0.55	0.725

The resolution limit is the resolution at which $\langle I/\sigma \rangle$ falls below 2. $\langle f_H \rangle / \langle E \rangle$, the phasing power, is calculated to 3 Å resolution. 21 732 unique reflections were collected on native crystal #2, which was the one used to obtain the experimental map used for fitting side chains. The data were 98% complete. Native #3, for which the data are similarly complete, was used for refinement.
$R_{sym} \equiv \Sigma |I_i - \langle I_i \rangle| / \Sigma I_i$; $R_F \equiv \Sigma |F_{deriv} - F_{native}| / \Sigma F_{native}$;
$\langle f_H \rangle / \langle E \rangle \equiv (\langle I_H \rangle)^{1/2} / (\langle \varepsilon^2 \rangle)^{1/2}$,
where ε is the lack of closure error and f_H is the calculated heavy atom structure factor amplitude (Blundell and Johnson, 1976).

Description of the molecule

EF-G–GDP is a five domain protein whose overall shape resembles a tadpole (Figure 2, left). The molecule is ~110 Å long from the top of its G domain 'head' to the tip of its domain 4 'tail'. Its N-terminal domain is a G nucleotide-binding domain, or G domain, like that of other members of the GTPase family, as sequence comparisons had suggested it would be (Bourne *et al.*, 1991). EF-G's other domains are designated 2–5, N-terminus to C-terminus. Secondary structure elements are identified by letters (helices) and numbers (strands of sheets), with subscripts for domain identification where necessary to avoid ambiguity. Figure 2, right, shows the protein's secondary structure in schematic form.

The topology of strands 1_G–5_G and helices A_G–D_G in the G domain of EF-G is identical to that of other G domains (see Figure 2, right), and its conserved sequences are found in the expected places (Bourne *et al.*, 1991). Like other G proteins, EF-G has sequence similarities to a large family of ATPases in two regions, the Walker A-box and the Walker B-box (Walker *et al.*, 1982). The A-box, or P loop, joins 1_G and A_G and includes a conserved GKT sequence. That sequence interacts with the α and β phosphates of GDP in EF-G in the same way as it does in other G proteins and in ATPases like recA (Story and Steitz, 1992), except for the ε amino group of K25, which hydrogen bonds to the hydroxyl group of T84 instead of the β phosphate of the GDP (Figure 3). The absence of that lysine–phosphate hydrogen bond could explain EF-G's unusually low affinity for G nucleotides, but the issue deserves further examination. The crystals studied

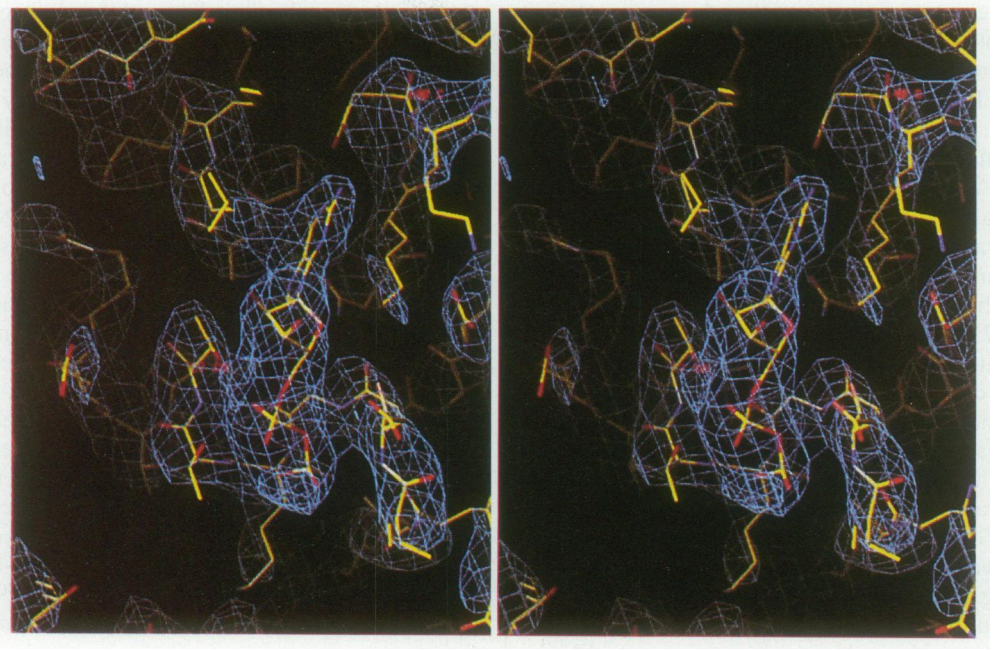

Fig. 1. Electron density in the GDP region. The experimentally phased electron density map in the region of the GDP binding site in EF-G, contoured at 1σ is shown in stereo with the current structure for EF-G–GDP superimposed.

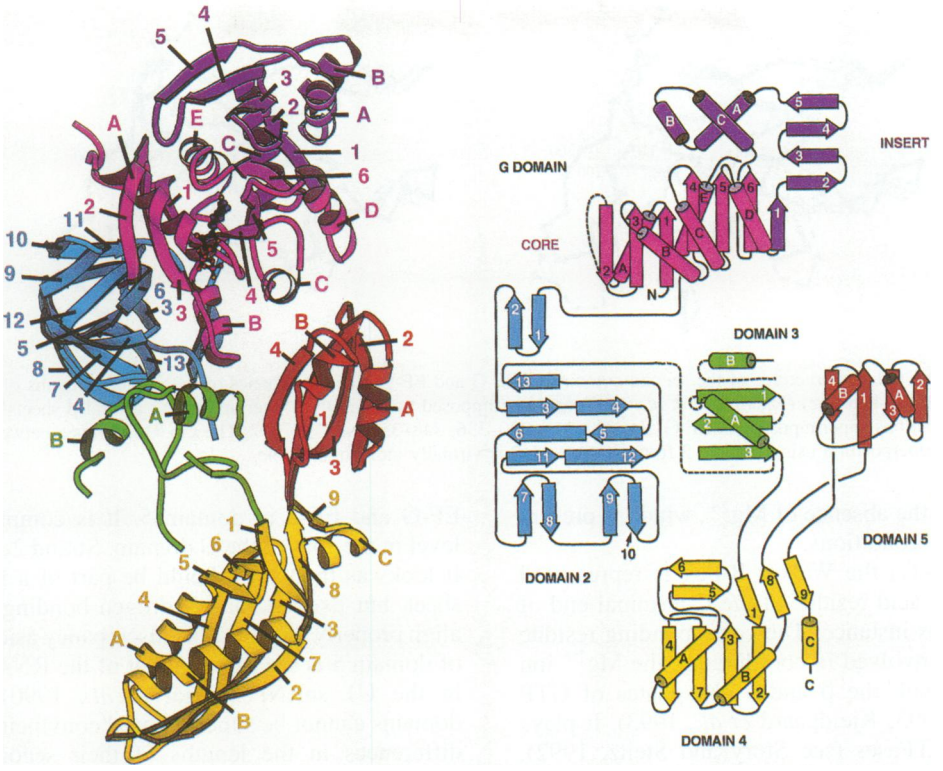

Fig. 2. Ribbon diagram of EF-G–GDP and its secondary structure. The left hand image is a MolScript (Kraulis, 1991) ribbon diagram of EF-G–GDP. The core of the G domain is light purple, and its insert is dark purple. Domain 2 is blue, while domain 3, which is poorly determined, is green. Domains 4 and 5 are yellow and red, respectively. Within each domain, helices are lettered A–Z, N-terminus to C-terminus, and strands are numbered 1 to n, in the same way. The bound GDP is shown in ball and stick format. The right hand image summarizes the secondary structure of EF-G. The alignment of secondary structure elements with the sequence is as follows. G domain core: begins at residue 1; 1, 11–16; A, 25–38; missing, 42–65; 2, 68–74; 3, 78–83; B, 92–100; 4, 103–108; C, 117–123; 5, 131–136; D, 146–155; G domain insert begins; 1, 161–164; 2, 167–169; 3, 176–178; 4, 184–188; 5, 196–198; A, 210–219; B, 225–232; C, 239–251; G core resumes; 6, 256–260; E, 269–279; G domain ends, 280. Domain 2: begins at 289; 1, 290–293; 2, 297–300; 3, 310–313; 4, 316–320; 5, 322–326; 6, 328–336; 7, 338–344; 8, 347–353; 9, 355–359; 10, 362–366; 11, 368–376; 12, 376–379; 13, 386–391; domain ends, 403. Domain 3: 404–482; 3, 477–481; backbone can be identified for an additional 64 residues. Domain 4: 1, 483–489; 2, 490–500; 3, 505–516; 4, 522–529; A, 539–550; 5, 551–553; 6, 557–559; 7, 563–571; B, 580–595; 8, 598–603; domain 4 interrupted by domain 5, 603; domain 4 resumes, 670; 9, 676–678; C, 681–689; sequence ends, 691. Domain 5: 1, 604–612; A, 617–623; 2, 630–634; 3, 642–647; B, 656–661; 4, 669–673; domain ends, 675. The registration between secondary structure elements and residue numbers is uncertain at the level of ±1 residue.

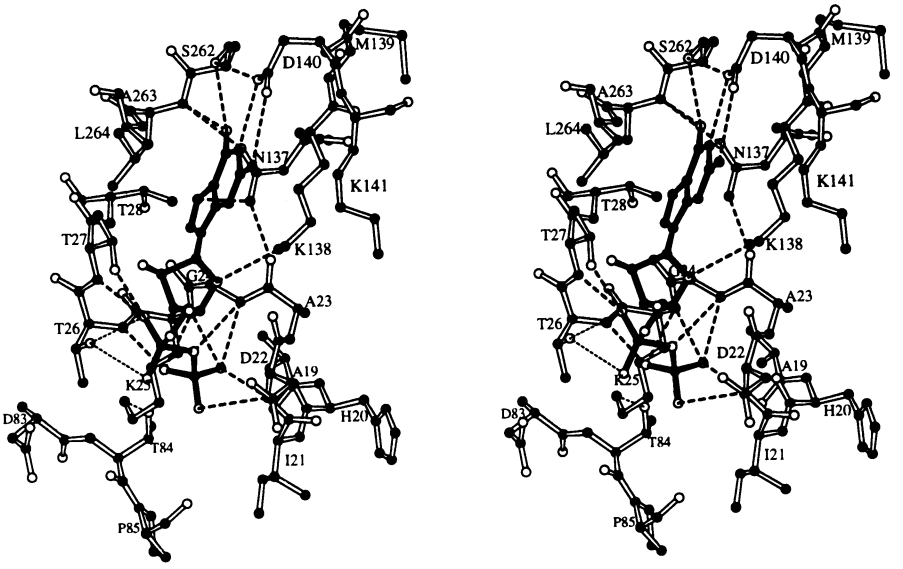

Fig. 3. Stereo view of the GDP binding site in EF-G. Oxygen atoms are white and all other atoms are black. Hydrogen bonds identical to those seen in EF-Tu–GTP (Berchtold *et al.*, 1993) are shown with heavy, broken lines. Hydrogen bonds unique to this molecule are shown using lighter broken lines.

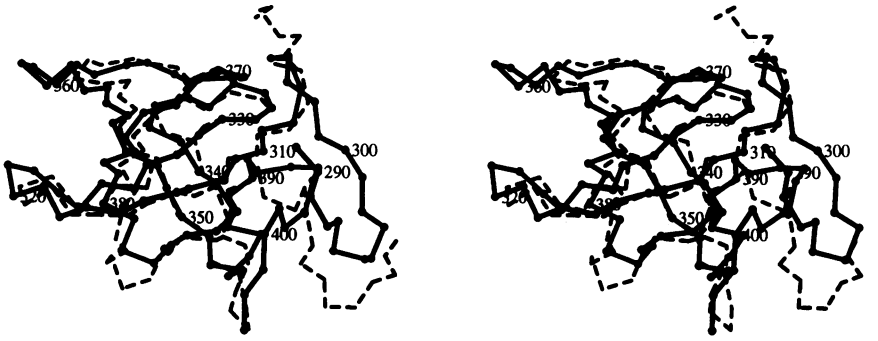

Fig. 4. Comparison of the tertiary structures of the second domains of EF-G and EF-Tu. The backbones of the second domains of EF-G–GDP (black) and EF-Tu–GTP (broken line) (Kjeldgaard *et al.*, 1993) are superimposed to maxmimize overlap in their central β sheets and shown in stereo. The Cα atom positions superimposed (in EF-G) are 309–316, 330–336, 348–353 and 367–377. The r.m.s. difference between superimposed atoms is 0.896 Å. The superposition using domain 2 from EF-Tu–GDP is virtually indistinguishable.

here were grown in the absence of Mg^{2+}, which is present under physiological conditions.

In EF-G and EF-Tu, the Walker B-box is represented by a single aspartic acid residue at the C-terminal end of strand 3, D83 in this instance. The corresponding residue in EF-Tu–GDP is involved in coordinating the Mg^{2+} ion that is associated with the β and γ phosphates of GTP (Berchtold *et al.*, 1993; Kjeldgaard *et al.*, 1993). It plays a similar role in ATPases (see Story and Steitz, 1992). D83's position in EF-G–GDP is not the same as in EF-Tu–GTP, but a modest conformational change in the 3_G–B_G region would bring it into line (see below).

The 'effector loop', or 'switch region' of EF-G (residues 42–65), whose position in other G proteins is affected by the γ phosphate of GTP (Bourne *et al.*, 1991), is disordered in EF-G–GDP. In addition, in comparison with EF-Tu, the connection between D_G and 6_G is augmented by a 90 residue insert, which is identified separately in Figure 2.

Domain 2 is a β sandwich that is strikingly similar to the second domain of EF-Tu in tertiary structure, except for its first two strands, which have no equivalents in EF-Tu (Figure 4) (Kjeldgaard and Nyborg, 1992; Berchtold *et al.*, 1993; Kjeldgaard *et al.*, 1993). The sequences of EF-G and EF-Tu are quite divergent in domain 2, however.

Domain 3 is an α–β domain, but the electron density map is so poor in this region that little more can be said, which is unfortunate because domain 3 is undoubtedly important functionally. The sequence similarity between EF-2 and EF-G in this 90 residue region—40% identity and 11% conservative substitutions (*Drosophila melanogaster* versus *Escherichia coli*)—is even higher than it is in the core of the G domain (Grinblat *et al.*, 1989; Cammarano *et al.*, 1992).

Domain 4, the tail of the molecule, is a well-ordered α–β domain. Its order may reflect crystal packing interactions. The most conspicuous intermolecular interaction in the crystal is a parallel interaction between strand $5_{G'}$ in one molecule and strand 4_4 of a neighbor, that merges the β sheet in the insert of one molecule with the β sheet in domain 4 of its neighbor. The helices in domain 4 are all on the same side of its sheet, as is the case with ribosomal proteins and other RNA binding domains, but its topology is unlike that of any known RNA binding protein.

Domain 5 is also an α–β domain. As in domain 3, there is a high level of sequence similarity between EF-G and EF-2 in domain 5. It is comparable with the level in the core of the G domain. Strand 2_5 is problematic. It looks as though it should be part of a four stranded β sheet, but its backbone hydrogen bonding groups do not align properly with 3_5. This discrepancy aside, the topology of domain 5 is the same as that of the RNA binding motif in the U1 snRNP (Nagai *et al.*, 1990), but the two domains cannot be superimposed convincingly because of differences in the lengths of their secondary structure elements.

It is particularly obvious from space filling models that the domains in EF-G group themselves into larger structures. The G domain and domain 2 constitute a single, large globular unit, while domains 4 and 5 look like a solid rod. Domain 3 is roughly spherical, and so placed that motions of the domain 4–5 rod relative to the globular G domain–domain 2 structure could hinge on it.

Comparisons with nucleotide-free EF-G and EF-Tu

When domains G, 2 and 4 of the Lund structure for nucleotide-free EF-G are superimposed on the corresponding domains of the Yale structure for EF-G–GDP, the r.m.s. difference between all Cα positions is 1.34 Å. This figure subsumes a 1–2° difference in angle between domain 4 and the G domain, and some localized, unresolved differences in sequence alignment. The r.m.s. difference in Cα positions in domain 5 is much larger, 3.09 Å. The reason is not that the electron density maps of the two proteins are so different in domain 5, but that the disorder in domain 5 is so high that the two groups have been unable to agree on how the sequence fits into it. The r.m.s. difference between Cα positions among residues involved in GDP binding (D22–T27, D83–P85 and N137–K141), on the other hand, is much smaller, 0.78 Å. The structures of EF-G and EF-G–GDP are closely similar.

The similarity of the second domains of EF-G and EF-Tu has already been noted. The G domains of the two proteins are also alike. The 16 Cα atoms in the P loop of EF-G–GDP (N14–T29) superimpose on the corresponding atoms of EF-Tu–GDP with a r.m.s.d. of 0.59 Å, and that superposition results in a close superposition of the rest of the nucleotide binding sites of both proteins.

Figure 5 compares the relative position of the G domain and second domain in EF-G–GDP with their relative positions in EF-Tu–GTP and in EF-Tu–GDP, which are quite different (Kjeldgaard and Nyborg, 1992; Berchtold

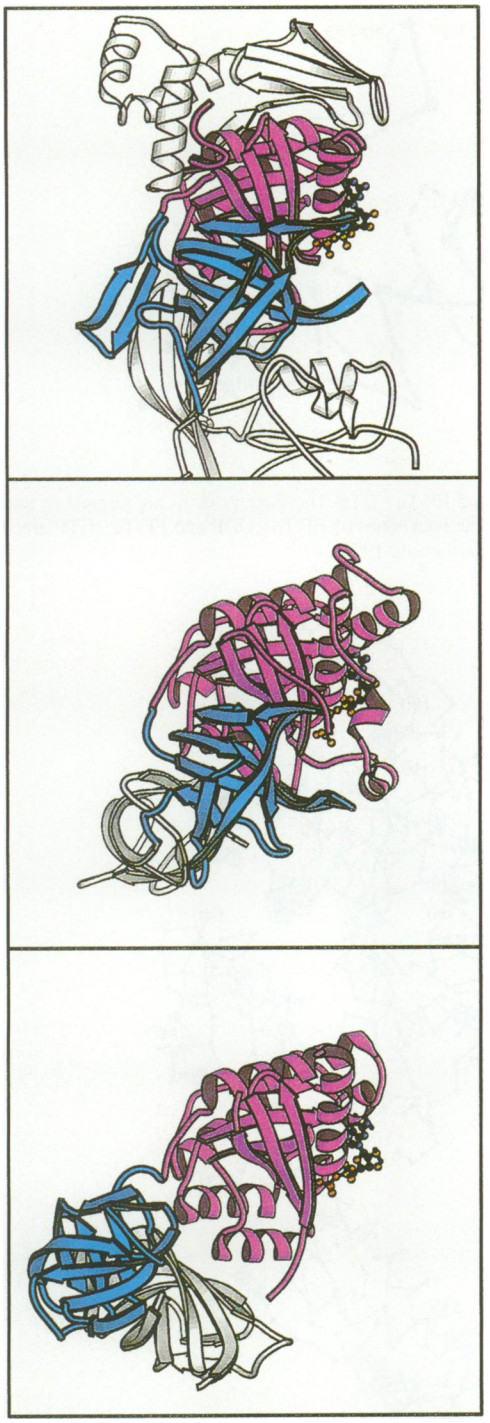

Fig. 5. The relative positions of the G domain and domain 2 in EF-G–GDP (top), EF-Tu–GTP (middle) and EF-Tu–GDP (bottom). The G domains (light purple) of all three proteins are oriented the same way by minimizing the differences between the α carbon positions of 58 residues in strands 1, 4, 5 and 6 of their G domains (Kjeldgaard and Nyborg, 1992; Kjeldgaard *et al.*, 1993). Second domains are blue. Other domains are gray.

et al., 1993; Kjeldgaard *et al.*, 1993). When the G domains of EF-G–GDP and EF-Tu–GTP are superimposed, the r.m.s. difference between α carbon atom positions in the strands of domain 2 is 3.4 Å. (The atoms compared are the ones superimposed in Figure 4.) The corresponding difference for EF-G–GDP versus EF-Tu–GDP is 20.7 Å. EF-G–GDP resembles EF-Tu–GTP, not EF-Tu–GDP.

The difference between EF-Tu–GDP and EF-Tu–GTP in the way domains are disposed is associated with a major difference in the position of helix B_G (Kjeldgaard and Nyborg, 1992; Berchtold *et al.*, 1993; Kjeldgaard *et al.*, 1993). It is interesting, therefore, to superimpose the nucleotide binding sites of the three proteins and then examine the placement of their B_G regions (Figure 6). Helix B_G in EF-G–GDP resembles helix B_G in EF-Tu–GTP more closely than it does helix B_G in EF-Tu–GDP, but the match is far from perfect.

Discussion

Since EF-Tu and EF-G are partly homologous, bind to the same site(s) on the ribosome and perform complementary functions, one might anticipate that their conformational responses to GTP cleavage would be similar. Why does EF-G–GDP resemble EF-Tu–GTP instead of EF-Tu–GDP? It could be that crystal packing forces stabilize non-physiological conformations of either EF-G–GDP or EF-Tu–GDP or EF-Tu–GTP, or some combination thereof. If the differences seen between the crystal structures are physiologically significant, however, we can conclude that the placement of second domains relative to G domains does not control the affinity of factors for the ribosome as such. EF-G–GDP, which has a low affinity for ribosomes, is like EF-Tu–GTP, which has a high affinity, but unlike EF-Tu–GDP, which is also low affinity (Spirin, 1985).

As is the case with many ATPases and GTPases, the hydrolysis of GTP by EF-G is not directly coupled to the conformational change it induces, i.e. translocation. Translocation occurs when EF-G–GTP interacts with pretranslocational ribosomes, independent of whether GTP hydrolysis ensues (Spirin, 1985). Non-hydrolyzable GTP analogs promote translocation but inhibit protein synthesis because EF-G is not released from the ribosome in their presence. Instead, GTP cleavage follows translocation, and is probably the consequence of a conformational alteration in the nucleotide binding site of EF-G, which results from translocation (see Nierhaus, 1993). The associated free energy change ensures that EF-G catalyzes the pre- to post-translocational transition, not its reverse. Once hydrolysis occurs, EF-G–GDP is released because EF-G in that conformation has a low affinity for ribosomes.

Since the structure of EF-G–GTP is unknown at this point, it is pointless to speculate about the conformational difference between it and EF-G–GDP. For reasons already discussed, however, it would not be surprising if it is significantly less dramatic than the one observed in EF-Tu (Berchtold *et al.*, 1993; Kjeldgaard *et al.*, 1993).

The properties of protein synthesis inhibitors that act by blocking EF-G fit well into the conceptual framework just outlined. Fusidic acid, for example, binds to the EF-G–GDP–ribosome complex (Willie *et al.*, 1975) and blocks elongation by preventing its dissociation. Since GTP hydrolysis follows translocation, a single translocation step ought to be possible in protein synthesizing systems poisoned by fusidic acid, and it is (Kaziro, 1978).

Fusidic acid could work by preventing the conformational change that normally follows GTP hydrolysis. If so, mutations to fusidic acid resistance should identify residues in EF-G's fusidic acid binding site and residues

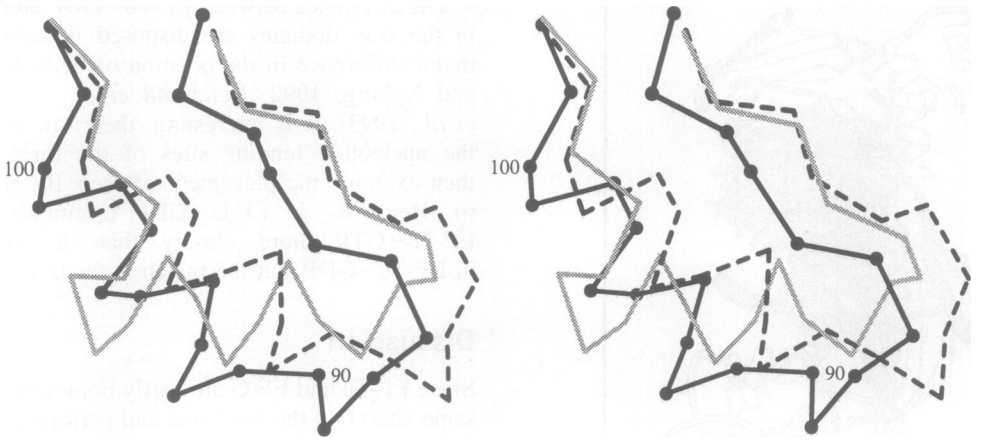

Fig. 6. The position of helix B_G in EF-G compared with its position in EF-Tu−GDP and EF-Tu−GTP. The three proteins are aligned so that their nucleotide binding sites are superimposed. The backbone of EF-G is shown in black. The backbones of EF-Tu−GDP and EF-Tu−GTP are shown in gray and with a broken black line, respectively (Kjeldgaard and Nyborg, 1992; Kjeldgaard *et al.*, 1993).

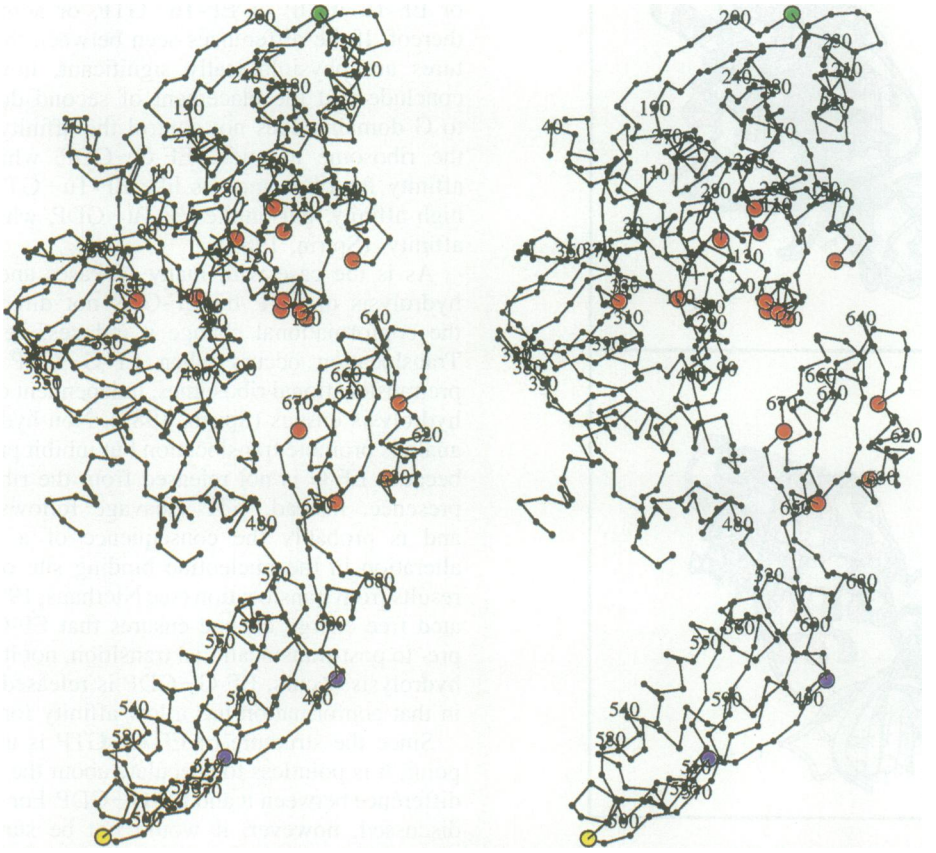

Fig. 7. The location of functionally significant sites in EF-G. The α carbon positions of mutant residues in fusidic acid resistant strains are red (Johanson and Hughes, 1994). Kanamycin resistant mutant sites are blue (Hou *et al.*, 1994). The approximate position of the residue altered when EF-2 is modified by diphtheria toxin is yellow (Robinson *et al.*, 1974) and the approximate position of the essential tryptophan in EF-2 is green (Guillot *et al.*, 1993).

important for EF-G's conformational change. Several fusidic acid resistant alleles of the gene for EF-G have been sequenced in *E.coli* recently (Johanson and Hughes, 1994). The residues altered fall in three groups when positioned in the structure. One group clusters on the side of the G domain facing domains 3 and 5 (Figure 7), and includes several residues on the side of C_G facing B_G. B_G plays a critical role in GTP driven conformational changes in other G proteins. The second set is found in domain 3; its members cannot be positioned in more detail at this point. The third group is found in domain 5. The mutated residues in C_G and one of the mutations in domain 5 (671) border a conspicuous gap between domain 5 and the G domain. One could imagine fusidic acid binding in this hole and inhibiting motions involving domains 3, 5 and the G domain.

Diphtheria toxin ADP-ribosylates a unique, modified histidine residue in mammalian EF-2, which is located at a position that corresponds approximately to D575 in *T.thermophilus* (see Figure 7) (Robinson *et al.*, 1974; Collier, 1975). Diphtheria toxin-treated EF-2 forms a ribosome–GTP complex, but neither translocation nor GTP cleavage ensues. The association of failure to translocate with failure to cleave GTP is consistent with the hypothesis that the latter depends on the former. The effect must be indirect; D575 is ~80 Å from the nucleotide binding site (in EF-G).

The inhibitory effect of diphtheria toxin can be explained by mechanistic models that postulate translocation dependent interactions between domain 4 and the 30S subunit (Traut *et al.*, 1986). For example, suppose the G domain of EF-G interacts with the 50S subunit in both pre- and post-translocational ribosomes (Liljas *et al.*, 1986; Moller and Maassen, 1986) and that domain 4 interacts with a site on the 30S subunit only after translocation. In that case, the 30S–domain 4 interaction would help drive translocation forward and could trigger GTP hydrolysis. The obvious place to look for the link between domain 4 and the nucleotide binding site, which might make the GTPase activity of EF-G depend on domain 4, runs through domain 5 and across the domain 5–G domain gap mentioned earlier. Indirect linkage through the ribosome cannot be ruled out, however.

Kanamycin causes a miscoding which can be overcome by mutations in EF-G. Recent sequencing results again point to the functional significance of domain 4. The residues altered in kanamycin-resistant forms of the EF-G gene in *E.coli* correspond to K489 and G495 in *Thermus* (Figure 7) (Hou *et al.*, 1994).

All large ribosomal subunits contain a highly conserved sequence called the sarcin–ricin loop because it is attacked by two protein toxins, α sarcin and ricin. Both inactivate ribosomes by cleaving a single covalent bond in the sarcin–ricin loop, which prevents their interaction with both EF-Tu and EF-G (Hausner *et al.*, 1987; Wool *et al.*, 1992). There is other evidence that the sarcin–ricin loop is part of the factor binding site (Moazed *et al.*, 1988). Many believe that translocation is triggered by the interaction of EF-G with the sarcin–ricin loop (Wool *et al.*, 1992; Nierhaus *et al.*, 1993).

Additional insight into the nature of the interaction of EF-G with the sarcin–ricin loop can be obtained from recent observations of Reboud and coworkers. They have shown that the interaction of EF-2 with the sarcin–ricin loop is affected by the oxidation of W221 (Guillot *et al.*, 1993). The sarcin–ricin loop is normally protected from α sarcin when EF-2 is bound. Oxidized EF-2 forms an EF-2–GTP–ribosome complex, but does not inhibit the activity of α sarcin, which implies a failure of the EF-2–sarcin–ricin interaction. Neither translocation nor GTP cleavage follows, as one would anticipate, if the sarcin–ricin loop plays the role suggested above. W221 is found in a region where the homology between EF-2 and EF-G is weak. It corresponds approximately to the loop that connects $5_{G'}$ and $A_{G'}$ (see Figure 6) (Cammarano *et al.*, 1992).

A number of residues have been identified in the G domain of EF-Tu that are involved in its interaction with EF-Ts (Arai *et al.*, 1974; Hwang *et al.*, 1992). While the search has been far from comprehensive, it is interesting that they all lie on a surface of the G domain of EF-Tu which would be concealed if the G domain of EF-Tu included the insert found in the G domain of EF-G. That same surface has been implicated in the interaction between $p21^{ras}$ and its GNRP (Bourne *et al.*, 1991). While it is certain that EF-Ts interacts with more than just the G domain of EF-Tu (Peter *et al.*, 1990), this correlation makes us wonder if the insert in EF-G's G domain has an EF-Ts-like function. Could it be that EF-G does not need a separate GNRP because it has one built-in?

Materials and methods

Purification of EF-G

EF-G was isolated from a thermophile believed to be *Thermus aquaticus* (YT-1) at the time the work began. Subsequent sequencing results leave little room for doubt, however, that it is *T.thermophilus* (HB8) (Drs Roland Kreutzer, Jutta Blank and Venkatraman Ramakrishnan, personal communications).

Thermus thermophilus was grown in ATCC medium 697 with Castenholz salts at 75°C and harvested in log phase. EF-G was purified using techniques adapted from published methods (Arai *et al.*, 1978; Leberman *et al.*, 1980). EF-G was precipitated from a postribosomal supernatant by addition of $(NH_4)_2SO_4$ to 65% saturation at 0°C. The protein pellet was dissolved in a minimal volume of Buffer B (50 mM Tris–HCl, 10 mM $MgCl_2$, 1 mM NaN_3, 0.5 mM DTT, 10 μM GDP and 10 μM PMSF, pH 7.6), dialyzed against Buffer B, and fractionated on DEAE–Sepharose CL-6B (Sigma/LKB-Pharmacia) with a gradient from 0.0 to 0.4 M NaCl in Buffer B. Fractions were assayed for GDP binding (Wurmbach and Nierhaus, 1979) and for ribosome-dependent GTPase activity (Leberman *et al.*, 1980). The fractions containing EF-G were pooled, precipitated with $(NH_4)_2SO_4$, dissolved in a minimal volume of Buffer B, and subjected to size-exclusion chromatography on Sephacryl S-200 (Sigma/LKB-Pharmacia) equilibrated with Buffer B. EF-G-containing fractions were pooled, concentrated and dialyzed against a solution of 5 mM sodium phosphate, 5 mM $MgCl_2$ and 1 mM DTT, pH 7.0. They were then loaded onto HA-Ultrogel (Sigma) column and eluted in a sodium phosphate gradient from 5 to 80 mM in the buffer used for dialysis. The final product was concentrated to 15.0 mg/ml and stored in 0.5 mM MOPS–NaOH, 2 mM DTT and 1 mM NaN_3, pH 7.6. The yield was ~15 mg of EF-G per 100 g of cells.

Preparation of EF-G crystals

Crystals were grown at room temperature in hanging drops containing 16–20% w/v PEG-8000 (Fischer) with 20 mM Tris–HCl, pH 7.8, 2 mM DTT, 1 mM GDP and 1mM NaN_3. After a crystal had grown to full size (0.3–1 mm long), the reservoir over which its drop was suspended was made 0.5% v/v in glutaraldehyde, and the cell was resealed. At least 8 h exposure to glutaraldehyde was necessary to prevent subsequent cracking (Quiocho and Richards, 1964). Longer exposure resulted in degradation of diffraction patterns. After glutaraldehyde treatment, crystals were suspended over stabilizing solution (30% w/v PEG-8000, 20 mM Tris–HCl, 20 mM ammonium acetate, 2 mM DTT, 1 mM GDP, 1 mM NaN_3, and in later experiments 100 mM NaCl) for ~24 h, then transferred directly into stabilizing solution.

Data collection and structure determination

All crystals were mounted in glass capillaries, and were maintained at room temperature (21°C) during data collection, except for the crystal that yielded native data set #3, which was kept at 4°C. Tetrakis(acetoxymercuri)methane, 3,5-dimercuri-4-dinitrophenol (DMNP), and Baker's dimercurial (1,4 diacetoxymercuri-2,3-dimethoxybutane) were used to make heavy atom derivatives.

X-ray diffraction data were collected on Xuong-Hamlin area detectors and a Rigaku R-Axis II imaging plate system. Data collected on the R-Axis system were integrated using DENZO (Z.Otwinowski) and scaled using SCALEPACK (Z.Otwinowski). Data collected on the Hamlin area detector were reduced with Hamlin software and scaled with SCALEPACK. Further processing was done using the CCP4 package of programs (SERC, 1979) . Heavy atom phases were refined using ML-PHARE (Otwinowski, 1991). SQUASH (Zhang, 1993) was used for phase improvement. Chain tracing and structural comparisons between

EF-G and EF-Tu, were done using the program O (Jones *et al.*, 1991). X-PLOR was used for refinement (Brunger *et al.*, 1987, Brunger, 1992).

Acknowledgements

The authors thank Professor Anders Liljas for making the backbone coordinates of nucleotide-free EF-G available to us prior to publication and for agreeing to publish his work simultaneously with ours. The EF-Tu coordinates used in this study were supplied by Dr Morten Kjeldgaard. We also wish to acknowledge Drs Jutta Blank and Roland Kreutzer for isolating the EF-G gene from our thermophile and informing us about their sequencing results. Dr V.Ramakrishnan supplied additional sequence information which helped in the identification of our organism. Ms Betty Freeborn provided technical help. This work was supported by grants from the National Institutes of Health (AI-09167 to P.B.Moore and GM22778 to T.A.Steitz and P.B.Moore).

References

Ævarsson,A., Brazhnikov,E., Garber,M., Zheltonosova,J., Chirgadze,Yu., Al-Karadaghi,S., Svensson,L.A. and Liljas,A. (1994) *EMBO J.*, **13**, 3669–3677.

Allende,J.E., Monro,R. and Lipmann,F. (1964) *Proc. Natl Acad. Sci. USA*, **51**, 1211–1216.

Arai,K., Kawaita,M., Nakamura,S., Ishikawa,I. and Kaziro,Y. (1974) *J. Biochem.*, **76**, 523–534.

Arai,K., Ota,Y., Arai,N., Nakamura,S., Henneke,C., Oshima,T. and Kaziro,Y. (1978) *Eur. J. Biochem.*, **92**, 509–519.

Arlinghaus,R., Shaeffer,J. and Schweet,R. (1964) *Proc. Natl Acad. Sci. USA*, **51**, 1291–1299.

Berchtold,H., Reshetnikova,L., Reiser,C.O.A., Schirmer,N.K., Sprinzl,M. and Hilgenfeld,R. (1993) *Nature*, **365**, 126–132.

Blundell,T.L. and Johnson,L.N. (1976) *Protein Crystallography*. Academic Press, London.

Bourne,H.R., Sanders,D.A. and McCormick,F. (1991) *Nature*, **349**, 117–127.

Brunger,A.T., Kuriyan,K. and Karplus,M. (1987) *Science*, **235**, 458–461.

Brunger,A.T. (1992) *X-PLOR Version 3.1. A System for X-ray Crystallography and NMR*. Yale University Press, New Haven, USA.

Cammarano,P., Palm,P., Creti,R., Ceccarelli,E., Sanangelantoni,A.M. and Tiboni,O. (1992) *J. Mol. Evol.*, **34**, 396–405.

Collier,R.J. (1975) *Bacteriol. Rev.*, **39**, 54–85.

Gavrilova,L.P., Kostiashkina,O.E., Koteliansky,V.E., Rutkevitch,N.M. and Spirin,A.S. (1976) *J. Mol. Biol.*, **101**, 537-552.

Grinblat,G., Brown,N.H. and Kafatos,F.C. (1989) *Nucleic Acids Res.*, **17**, 7303–7314.

Guillot,D., Lavergne,J.P. and Reboud,J.P. (1993) *J. Biol. Chem.*, **268**, 26082–26084.

Gupta,S.L., Waterson,J., Sopori,M.L., Weissman,S.M. and Lengyel,P. (1971) *Biochemistry*, **10**, 4410–4421.

Hausner,T.P., Atmadja,J. and Nierhaus,K.H. (1987) *Biochimie*, **69**, 911–923.

Hou,Y., Lin,Y.P., Sharer,J.D. and March,P.E. (1994) *J. Bacteriol.*, **176**, 123–129.

Hwang,Y.W., Carter,M. and Miller,D.L. (1992) *J. Biol. Chem.*, **267**, 22198–22205.

Johanson,U. and Hughes,D. (1994) *Gene*, **143**, 55–59.

Jones,T.A., Cowan,S., Zou,J.Y. and Keldgaard,M. (1991) *Acta Crystallogr.*, **A46**, 110–119.

Kaziro,Y. (1978) *Biochim. Biophys. Acta*, **505**, 95.

Kjeldgaard,M. and Nyborg,J. (1992) *J. Mol. Biol.*, **223**, 721–742.

Kjeldgaard,M., Nissen,P., Thirup,S. and Nyborg,J. (1993) *Structure*, **1**, 35–50.

Kraulis,P.J. (1991) *J. Appl. Crystallogr.*, **24**, 946–950.

Leberman,R., Antonsson,B., Giovanelli,R., Guariguata,R., Schumann,R. and Wittinghofer,A. (1980) *Anal. Biochem.*, **104**, 29–36.

Liljas,A., Kirsebom,L.A. and Leijonmarck,M. (1986) In Hardesty,B. and Kramer,G. (eds), *Structure, Function and Genetics of Ribosomes*. Springer Verlag, New York, pp. 379–390.

Moazed,D., Roberston,J.M. and Noller,H.F. (1988) *Nature*, **334**, 362–364.

Moller,W. and Maassen,J.A. (1986) In Hardesty,B. and Kramer,G. (eds), *Structure, Function, and Genetics of Ribosomes*. Springer Verlag, New York, pp. 309–325.

Nagai,K., Oubridge,C., Jessen,T.H., Li,J. and Evans,P.R. (1990) *Nature*, **348**, 515–520.

Nathans,D. and Lipmann,F. (1961) *Proc. Natl Acad. Sci. USA*, **47**, 497–504.

Nierhaus,K.H. (1993) *Mol. Microbiol.*, **9**, 661–666.

Nierhaus,K.H., Adlung,T.P., Hausner,S., Schilling Bartetzko,S., Twardowski,T. and Triana,F. (1993) In Nierhaus,K.H., Franceschi,F., Subramanian,A.R., Erdmann,V.A. and Wittmann Liebold,B. (eds), *The Translational Apparatus*. Plenum Press, New York, pp. 263–272.

Nizushima,Y. and Lipmann,F. (1966) *Proc. Natl Acad. Sci. USA*, **55**, 212–219.

Otwinowski,Z. (1991) *ML-PHARE CCP4 Proc. 80–88*. Daresbury Laboratory, Warrington, UK.

Peter,M.E., Reiser,C.O.A., Schirmer,N.K., Kiefhaber,T., Ott,G., Grillenbeck,N.W. and Sprinzl,M. (1990) *Nucleic Acids Res.*, **18**, 6889–6893.

Quiocho,F.A. and Richards,F.M. (1964) *Proc. Natl Acad. Sci. USA*, **52**, 833–839.

Rheinberger,H.J., Geigenmuller,U., Gnirke,A., Hausner,T.P., Remmer,J., Saruyama,H. and Nierhaus,K.H. (1990) In Hill,W.E., Dahlberg,A., Garrett,R.A., Moore,P.B., Schlessigner,D. and Warner, J.R. (eds), *The Ribosome, Structure, Function and Genetics*. American Society for Microbiology, Washington, DC, pp. 318–330.

Richman,N. and Bodley,J.W. (1972) *Proc. Natl Acad. Sci. USA*, **69**, 686–689.

Robinson,E.A., Henriksen,O. and Maxwell,E.S. (1974) *J. Biol. Chem.*, **249**, 5088–5093.

Schilling Bartetzko,S., Bartetzko,A. and Nierhaus,K.H. (1992) *J. Biol. Chem.*, **267**, 4703–4712.

SERC (1979) *CCP4*. Daresbury Laboratory, Warrington, UK.

Spirin,A.S. (1985) *Progr. Nucleic Acid Res. Mol. Biol.*, **32**, 75–114.

Story,R.M. and Steitz,T.A. (1992) *Nature*, **355**, 374–376.

Thach,S.S. and Thach,R.E. (1971) *Proc. Natl Acad. Sci. USA*, **68**, 1791–1795.

Traut,R.R., Tewari,D.S., Sommer,A., Gavino,G.R., Olson,H.M. and Glitz,D.G. (1986) In Hardesty,B. and Kramer,G. (eds), *Structure, Function and Genetics of Ribosomes*. Springer Verlag, New York, pp. 286–308.

Walker,J.E., Saraste,M., Runswick,M.J. and Gay,N. (1982) *EMBO J.*, **1**, 945–951.

Wang,B.C. (1985) *Methods Enzymol.*, **115**, 90–112.

Willie,G.R., Richman,N., Godtfredsen,W.O. and Bodley,J.W. (1975) *Biochemistry*, **14**, 1713–1718.

Wool,I.G., Gluck,A. and Endo,Y. (1992) *Trends Biochem. Sci.*, **17**, 266–269.

Wurmbach,P. and Nierhaus,K.H. (1979) *Methods Enzymol.*, **60**, 593–606.

Yaknin,A.V., Vorozheykina,D.P. and Matvienko,N.I. (1989) *Nucleic Acids Res.*, **17**, 8863.

Zhang, K.Y.J. (1993) *Acta Crystallogr.*, **D49**, 213–222.

Received on 9 May, 1994